

Y-branch integrated dual wavelength laser diode for microwave generation by sideband injection locking

Jin Huang, Changzheng Sun*, Bing Xiong and Yi Luo

State Key Laboratory on Integrated Optoelectronics, Tsinghua National Laboratory for Information Science and Technology, Department of Electronic Engineering, Tsinghua University, Beijing 100084, P. R. China
*czsun@tsinghua.edu.cn

Abstract: A Y-branch integrated dual wavelength laser diode is fabricated for optical microwave generation based on the principle of sideband injection locking. The device integrates a master laser and a slave laser with associated Y-branch coupler. By directly modulating the master laser near its relaxation resonance frequency, multiple sidebands are generated due to enhanced modulation nonlinearity. Beat signal with high spectral purity is obtained by injection locking the slave laser to one of the modulation sidebands. A millimeter-wave carrier of 42-GHz with a phase noise of -94.6 dBc/Hz at 10 kHz offset is demonstrated.

©2009 Optical Society of America

OCIS codes: (060.4510) Optical communications; (140.5960) Semiconductor lasers.

References and links

1. K. Kitayama, "Architectural considerations of fiber-radio millimeter-wave wireless access systems," *Fiber Integr. Opt.* **19**(2), 167–186 (2000).
2. A. J. Seeds, and K. J. Williams, "Microwave photonics," *J. Lightwave Technol.* **24**(12), 4628–4641 (2006).
3. M. Ogusu, K. Inagaki, and T. Ohira, "Subcarrier multiplexing signal modulation at 60 GHz using two-mode injection-locked Fabry-Perot laser," *Electron. Lett.* **36**(25), 2102–2103 (2000).
4. S. Bauer, O. Brox, J. Kreissl, G. Sahin, and B. Sartorius, O. Brox, J. Kreissl, G. Sahin, and B. Sartorius, "Optical microwave source," *Electron. Lett.* **38**(7), 334–335 (2002).
5. R. P. Braun, G. Grosskopf, D. Rohde, and F. Schmidt, "Low-phase-noise millimeter-wave generation at 64 GHz and data transmission using optical sideband injection locking," *IEEE Photon. Technol. Lett.* **10**(5), 728–730 (1998).
6. M. Ogusu, K. Inagaki, and Y. Mizuguchi, "60 GHz millimeter-wave source using two-mode injection-locking of a Fabry-Perot slave laser," *IEEE Microw. Wirel. Compon. Lett.* **11**(3), 101–103 (2001).
7. C. Laperle, M. Svilans, M. Poirier, and M. Têtu, "Frequency multiplication of microwave signals by sideband optical injection locking using a monolithic dual-wavelength DFB laser device," *IEEE Trans. Microw. Theory Tech.* **47**(7), 1219–1224 (1999).
8. D. Y. Kim, M. Pelusi, Z. Ahmed, D. Novak, H. F. Liu, and Y. Ogawa, "Ultrastable millimetre-wave signal generation using hybrid modelocking of a monolithic DBR laser," *Electron. Lett.* **31**(9), 733–734 (1995).
9. L. A. Johansson, and A. J. Seeds, "Millimeter-wave modulated optical signal generation with high spectral purity and wide-locking bandwidth using a fiber-integrated optical injection phase-lock loop," *IEEE Photon. Technol. Lett.* **12**(6), 690–692 (2000).
10. L. Chen, Y. Pi, H. Wen, and S. Wen, "All-optical mm-wave generation by using direct-modulation DFB laser and external modulator," *Microw. Opt. Technol. Lett.* **49**(6), 1265–1267 (2007).
11. T. Wang, M. Chen, H. Chen, J. Zhang, and S. Xie, "Millimeter-wave signal generation using two cascaded optical modulators and FWM effect in semiconductor optical amplifier," *IEEE Photon. Technol. Lett.* **19**(16), 1191–1193 (2007).
12. R. P. Braun, G. Grosskopf, R. Meschenmoser, D. Rohde, F. Schmidt, and G. Villino, "Microwave generation for bidirectional broadband mobile communications using optical sideband injection locking," *Electron. Lett.* **33**(16), 1395–1396 (1997).
13. J. Huang, C. Sun, Y. Song, B. Xiong, and Y. Luo, "Influence of master laser's lineshape on the optically generated microwave carrier by injection locking," *Appl. Phys. Express* **2**, 072502 (2009).
14. K. Petermann, *Laser Diode Modulation and Noise*, (Kluwer, Dordrecht, 1991).

1. Introduction

Millimeter-wave (mm-wave) communication is considered as a promising approach for future broadband wireless access system due to its wide bandwidth, reuse of frequency band, good

confidentiality, and so on [1]. However, mm-wave communication system based on electrical devices suffers from disadvantages including high cost, high transmission loss and electromagnetic interference. Therefore, radio over fiber (RoF) systems which adopt optical technique to generate and transmit mm-wave signal have been proposed and studied extensively during the past few years [2–4]. One of the key issues in RoF systems is to optically generate mm-wave carriers with high spectral purity. Many techniques for mm-wave optical generation have been proposed, for instance, sideband injection locking [5–7], mode-locked lasers [8], optical phase locking loop [9], and external modulation [10,11].

Among the various methods mentioned above, sideband injection locking is able to generate microwave carriers with high spectral purity and has exhibited high stability and tunability for the carriers [12]. However, spectral purity of microwave carrier generated by sideband injection locking using discrete devices often suffers from decorrelation due to optical path difference between the two beating lights [13]. A possible solution to this problem is monolithically integrating the master laser and the slave laser on a single chip. Because of the compact size of the monolithically integrated device, optical path difference between the two beating lights is negligible. Meanwhile, monolithically integrated device also greatly reduces the system complexity and cost compared to microwave generation systems based on discrete devices.

In this letter, we present a Y-branch integrated dual wavelength laser diode for optical microwave generation, which contains a master laser (ML) and a slave laser (SL) as well as a Y-branch coupler. The ML is directly modulated near its relaxation resonance frequency to generate high order sidebands due to enhanced nonlinearity of modulation response. When the SL is injection locked to one of the modulation sidebands of the ML, mm-wave carrier with high spectral purity at eight times the modulation frequency can be generated.

2. Device design and fabrication

Figure 1(a) presents the schematic diagram of the Y-branch integrated dual wavelength laser diode. The device consists of two distributed feedback (DFB) lasers and one Y-branch section monolithically integrated on the same AlGaInAs multiple quantum well (MQW) active layer. One of the DFB lasers works as the ML and is directly modulated, while the other one works as the SL. Light injection from the ML into the SL is realized by reflection at the end facet of the Y-branch section. The injection level can be controlled by adjusting the current of the Y-branch section, which can affect the tuning range of the generated microwave. Higher injection level will result in a larger tuning range.

The device is completed with a two-step growth by metal organic chemical vapor-phase deposition (MOCVD). During the first growth, an n-InP buffer layer, an InAlAs lower cladding layer, an MQW active layer, and an InAlAs upper cladding layer are grown on the n⁺-InP substrate. The MQW structure consists of 10 pairs of 6-nm-thick compressively-strained AlGaInAs well and 10-nm thick tensile-strained AlGaInAs barrier, sandwiched between two 35-nm-thick undoped graded-index (GRIN) AlGaInAs layers. In addition, a 30-nm p-InP spacer layer, a 10-nm p-InGaAsP etch-stop layer, a 70-nm p-InP layer, and a 20-nm p-InGaAsP grating layer are also grown on top of the upper cladding layer during the first growth. A first-order grating is formed in the DFB laser section by holographic exposure followed by chemical etching in HBr:HNO₃:H₂O solution. During the second growth, a 1.3- μ m p-InP layer and a 0.2- μ m p⁺-InGaAs contact layer are grown successively over the wafer.

After the MOCVD regrowth, the wafer is processed into device chips. The lengths of the DFB laser section and the Y-branch section are designed to be 420 and 400 μ m, respectively. The DFB lasers and the Y-branch are all processed into ridge waveguide structure. The ridge width is 2 μ m and the ridge depth is about 1.5 μ m, as controlled by the etch-stop layer above the active layer. In order to reduce the propagation loss as much as possible, the transition waveguide of the Y-branch is designed to have a radius of curvature of 11.46 mm and the angle between the two DFB lasers is 4°. The smallest distance between the two DFB lasers is 14 μ m, which ensures that there is no mode coupling between them. A 250-nm-thick SiO₂ insulation layer is then deposited on top of the wafer by plasma-enhanced chemical vapor-

phase deposition (PECVD) and the SiO_2 film on top of the ridge waveguide is removed by buffered HF solution with a self-aligned lithography.

Cr/Au p-electrode is then formed on top of the wafer by sputtering. Electrical isolation between the DFB lasers and the Y-branch is realized by removing the electrode and the ohmic contact layer in the isolation region. Ti/Au n-electrode is sputtered onto the backside of the device after thinning the wafer down to about 120 μm . The wafer is then cleaved into device chips, and both facets of the device are left as cleaved. Figure 1(b) shows the photograph of the fabricated device.

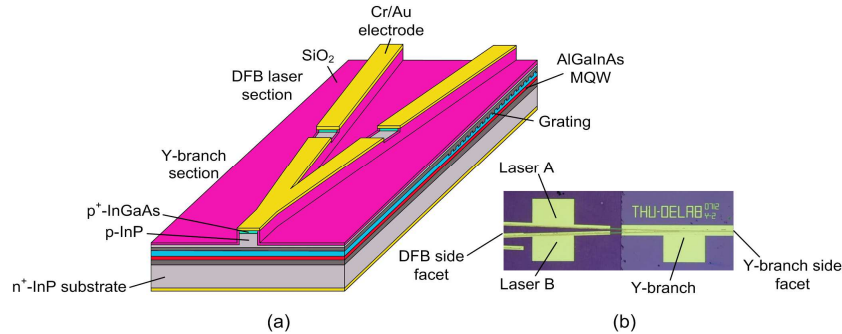


Fig. 1. (a) Schematic diagram and (b) photograph of the Y-branch integrated dual wavelength laser diode for microwave generation.

The device chip is then bonded p-side up onto an alumina submount and attached to a Cu heat sink, whose temperature is maintained at 25°C with a Peltier effect cooler. The threshold current of the DFB lasers of the integrated device is around 17 mA, when the Y-branch section is unbiased. For convenience, the two DFB lasers will hereafter be labeled as A and B, respectively. Figure 2 depicts the lasing spectrum measured at the Y-branch facet, when the injection currents of laser A, laser B, and Y-branch section are 28, 35, and 30 mA, respectively. The wavelength difference between the two DFB lasers is 218 pm, which can be tuned by varying the heat sink temperature or by adjusting the injection currents of the DFB lasers as well as the Y-branch section. In addition, the linewidth of each DFB laser is measured to be about 6 MHz.

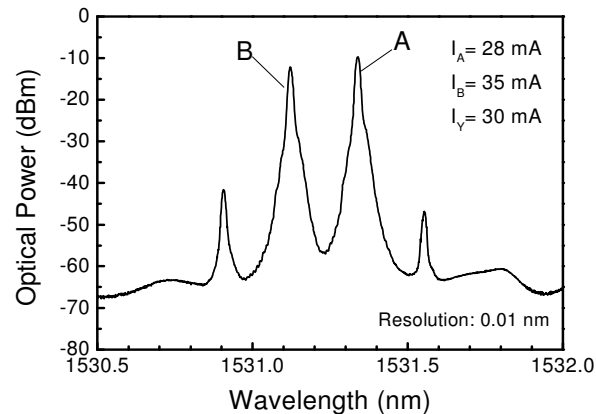


Fig. 2. Lasing spectrum of the Y-branch integrated dual wavelength laser diode.

3. Microwave generation

For optical generation of microwave signal, one of the two DFB lasers in the Y-branch integrated dual wavelength laser diode works as the ML and the other one works as the SL. When the injection current of the ML is modulated at a frequency f , a series of sidebands will

be generated on both sides of the optical carrier due to amplitude modulation (AM) and frequency modulation (FM) [14]. If the SL is injection locked to the $+n$ -th sideband, microwave carrier at a frequency of $(n+m)f$ will be generated by heterodyning the SL with the $-m$ -th sideband of the ML, which is easily implemented with a high-speed photodetector (PD). In this way, frequency multiplication is accomplished. To generate mm-wave carrier from low frequency RF signal, the key point is to generate high order modulation sidebands, which can be realized by taking advantage of the enhanced AM and FM response around the relaxation resonance frequency of the ML.

3.1 Direct modulation of ML near its relaxation resonance frequency

In the following experiments, laser B is chosen as the ML, whereas laser A acts as the SL. The modulation response of laser B is measured with an Agilent 8722ET network analyzer to determine its relaxation resonance frequency. A microwave probe is used to feed the sweep frequency signal from the network analyzer to the electrode of laser B, and the output light exiting the DFB side facet is detected by a high-speed PD. The frequency response shown in Fig. 3 indicates a relaxation resonance frequency of 5.95 GHz for laser B at an injection current of 35 mA.

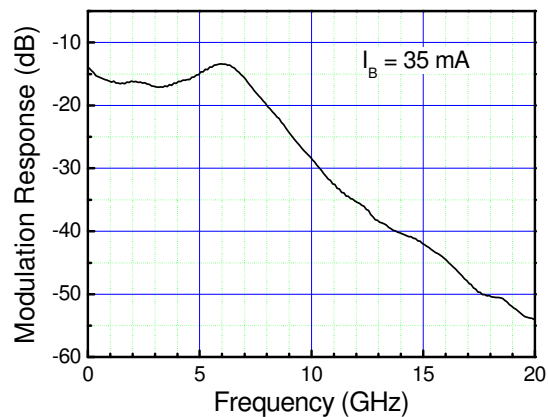


Fig. 3. Small-signal modulation response of laser B biased at 35 mA.

Figure 4 shows the optical spectra of laser B modulated at different modulation frequencies, when the RF power of the modulation signal is kept at 5 dBm. At a modulation frequency of 6 GHz, which is close to the relaxation resonance frequency of the laser, quite a number of sidebands are generated with intensity comparable to that of the optical carrier. On the other hand, when the laser is modulated at 9 GHz, a frequency much higher than the relaxation resonance frequency, only a limited number of sidebands with reduced intensity can be observed. The difference is attributed to the enhanced nonlinearity of modulation response around the relaxation resonance frequency of the laser [14].

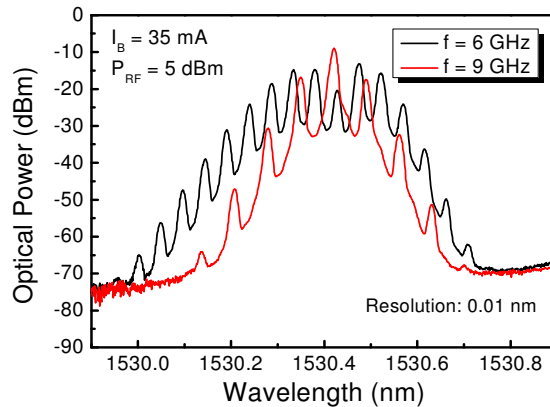


Fig. 4. Optical spectra of laser B at different modulation frequencies when biased at 35 mA.

3.2 Microwave generation by sideband injection locking

Microwave generation is then carried out by using the Y-branch integrated dual wavelength laser diode. The schematic diagram of the experimental setup is shown in Fig. 5. The temperature of the device is stabilized at 25°C. The ML (laser B) is biased at I_B and driven by an Agilent E8257D microwave signal generator via a bias Tee. The SL (laser A) and Y-branch section are DC biased at I_A and I_Y , respectively. A tapered single-mode fiber is used to couple the light output at the Y-branch facet into a 50-GHz PD (u^t XPDV2020) by way of a 50/50 fiber coupler. The beat signal is recorded by an Agilent E4446A electrical spectrum analyzer (ESA). The light going through the other arm of the 50/50 coupler is monitored by an Ando AQ6317B optical spectrum analyzer (OSA).

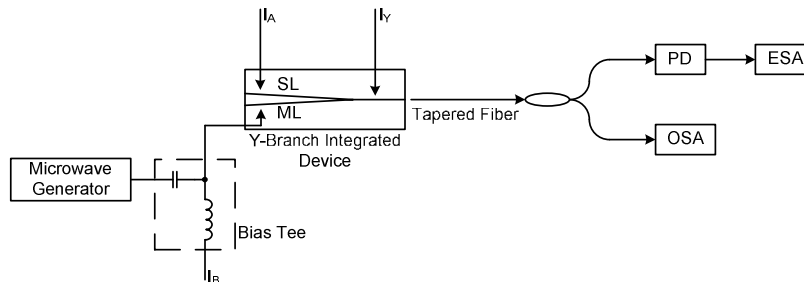


Fig. 5. Schematic diagram of the experimental setup. ML: master laser; SL: slave laser; PD: photodetector; ESA: electrical spectrum analyzer; OSA: optical spectrum analyzer.

In the experiment, the DC bias current of the ML is set to be $I_B = 35$ mA. The frequency and the RF power of the modulation signal applied to the ML are $f = 5.25$ GHz and $P_{RF} = 10$ dBm, respectively. By tuning the injection current of the SL and the Y-branch section to $I_A = 28$ mA and $I_Y = 30$ mA, respectively, the SL is locked to one of the high order modulation sidebands due to reflection at the Y-branch facet. Figure 6 shows the optical spectrum of light exiting the Y-branch facet, where a series of sidebands with similar peak intensity are generated due to direct modulation of the ML around its relaxation resonance frequency. The heterodyning spectra recorded by the ESA are shown in Fig. 7. When the ML is not under modulation, and both the ML and the SL are in free-running state, a Lorentzian-shaped peak can be observed around 27 GHz, as shown in Fig. 7(a). The full-width-at-half-maximum (FWHM) linewidth of the beat signal is on the order of 10 MHz, due to the lack of phase-correlation between the two lasers. This is in agreement with the measured linewidth of DFB lasers under similar bias current. The spectrum shown in Fig. 7(b) corresponds to the case when laser B is under modulation, while laser A is unbiased. Peaks at multiples of the

modulation frequency f can be observed, but their intensity decreases rapidly at high frequencies. On the other hand, when laser A is locked to one of the modulation sidebands of laser B, mm-wave carrier at frequency over 40 GHz can be clearly observed, as shown in Fig. 7(c). In our experiment, due to the bandwidth limit of the ESA, carrier with a frequency up to 42 GHz is recorded, corresponding to 8-times the modulation frequency. In a practical system built around this device, the beat signal at aimed frequency can be selected by a microwave filter.

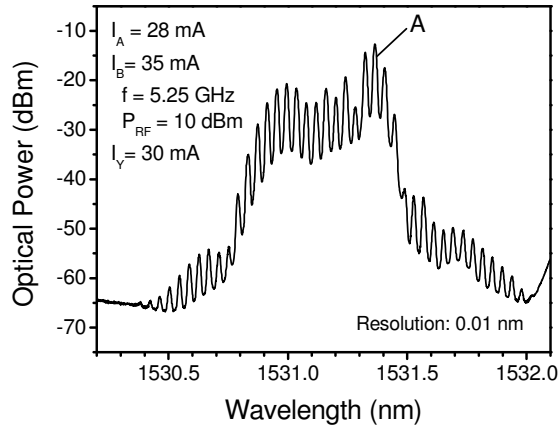


Fig. 6. Optical spectrum of the Y-branch integrated dual wavelength laser diode when the SL is locked to one of the sidebands of the ML.

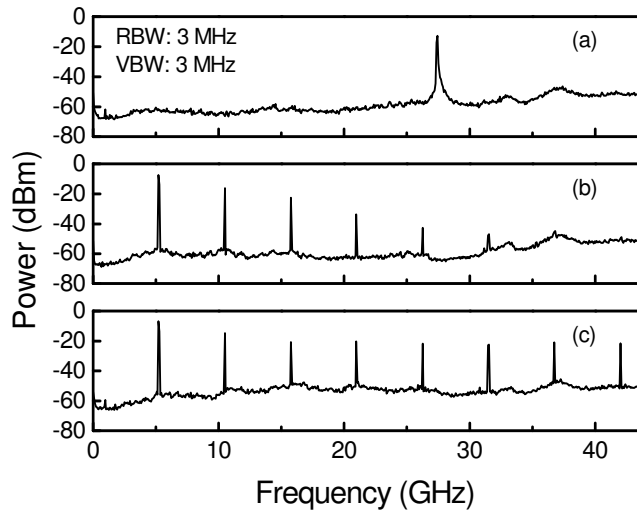


Fig. 7. Electrical spectra measured at the Y-branch facet (a) both DFB lasers in free-running state without modulation; (b) laser B modulated at 5.25 GHz, laser A unbiased; (c) laser B under modulation, laser A locked to one of the sidebands.

Figure 8 gives the electrical spectrum of the 42-GHz mm-wave carrier generated with the Y-branch integrated dual wavelength laser diode. High spectral purity is obtained due to the correlation between the ML and the SL upon injection locking. The power of the 42-GHz carrier is -23.7 dBm, which is limited by the optical power coupled into the PD and the responsivity of the PD at this frequency. It should be noted that, unlike the case reported in Ref [7], no Lorentzian-shaped noise floor is observed around the 42-GHz beat signal, indicating excellent correlation between the two lasers. The phase noise of the 42-GHz mm-

carrier is plotted in Fig. 9. A phase noise of -94.6 dBc/Hz at 10 kHz offset and -98.5 dBc/Hz at 100 kHz offset is demonstrated. For comparison, the phase noise of the modulation signal at 5.25 GHz is also plotted in Fig. 9. It is seen that, compared with the modulation signal, the phase noise of optically generated 42-GHz mm-wave carrier exhibits only about 18 dB degradation, which is in accord with 8-time frequency multiplication.

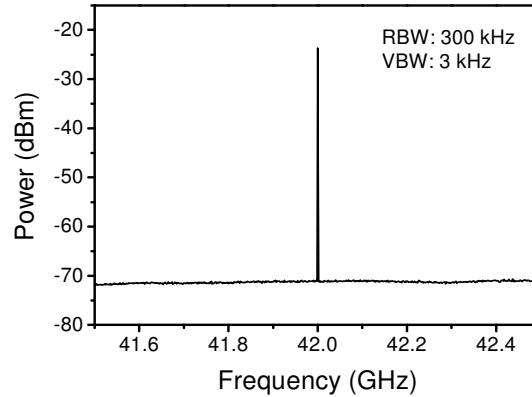


Fig. 8. Electrical spectrum of the generated 42-GHz microwave carrier.

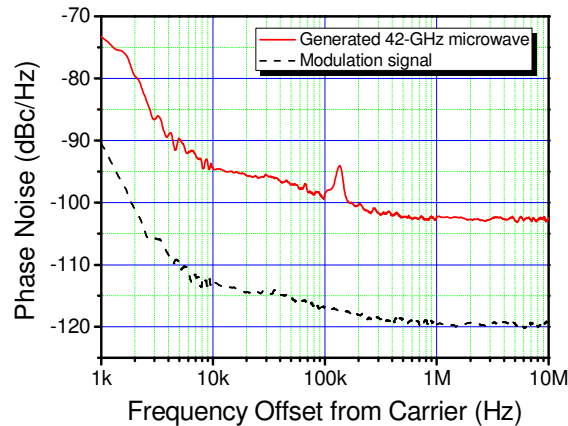


Fig. 9. Phase noise spectra of the optically generated 42-GHz carrier and the modulation signal.

The frequency of the generated mm-wave carrier can be easily tuned by varying the modulation signal around the relaxation resonance frequency of the ML and adjusting the SL current accordingly. A tuning range of over 450 MHz can be realized by adjusting only the modulation frequency of the ML. On the other hand, a tuning range of over 4 GHz is demonstrated by adjusting the bias currents of the lasers as well as the modulation frequency. In addition, no significant variation in the RF power and spectral purity of the mm-wave carrier is observed within the tuning range. By improving the DFB laser structure, relaxation resonance frequency in excess of 10 GHz can be realized. As a result, the Y-branch integrated dual wavelength laser diode is believed to have promising potential in 60 GHz mobile communication systems.

4. Conclusion

A Y-branch integrated dual wavelength laser diode has been fabricated to generate mm-wave signal based on sideband injection locking. The device contains two DFB lasers and a Y-branch coupler. By modulating one of the DFB lasers near its relaxation resonance frequency, multiple sidebands are generated due to the enhanced modulation response nonlinearity. Mm-

wave carrier with high spectral purity is obtained by locking the other laser to one of the high-order modulation sidebands. Frequency multiplication up to 8 times of the modulation frequency has been demonstrated, and 42.0-GHz beat signal with a phase noise of -94.6 dBc/Hz at 10 kHz offset is generated. The Y-branch integrated dual wavelength laser diode exhibits great potential in future mm-wave mobile communication system.

Acknowledgments

This work was supported in part by the National Natural Science Foundation of P. R. China (Nos. 60536020, 50706022, 60723002, and 60977022), and the “973” Major State Basic Research Development Program of China (Nos. 2006CB302800 and 2006CB921106).